INSTITUTE OF PHYSICS PUBLISHING JOURNAL OF PHYSICS: CONDENSED MATTER

J. Phys.: Condens. Matter **15** (2003) S479–S494 PII: S0953-8984(03)55333-4

Interlayer exchange coupling and giant magnetoresistance

Peter Weinberger[1] **and Laszlo Szunyogh**[1,2]

[1] Center for Computational Materials Science, Getreidemarkt 9/134, A-1060 Vienna, Austria
[2] Department of Theoretical Physics, Budapest University of Technology and Economics, Budafoki út. 8, 1521 Budapest, Hungary

Received 29 October 2002
Published 27 January 2003
Online at stacks.iop.org/JPhysCM/15/S479

Abstract

Starting from an algebraic description of collinearity within density functional theory the concept of magnetic configurations is introduced, which in turn is of crucial importance to define the interlayer exchange energy (IEC) and the (giant) magnetoresistance (GMR). The applications shown are meant to clarify not only the conceptual basis of IEC and GMR, but also the difficulties that can arise in actual calculations.

1. Introduction

Right from the beginning, i.e., right after their discoveries, interlayer exchange coupling (IEC) and giant magnetoresistance (GMR) were considered to be just two sides of one coin or at least twins, as far as the oscillations with respect to the number of spacer layers and other properties are concerned. Perhaps one of the starting points for this conception was a paper describing a two-monolayer periodicity of the oscillations in the magnetoresistance of Fe/Cr/Fe trilayers [1]. There results of Kerr and magnetoresistance measurements were put in one and the same figure, and, alas, their peak positions at least up to a spacer thickness of about 15–20 Å coincided. Many papers before and even more investigations after publication of this paper dealt with all kinds of effect of either the IEC or the GMR. In particular the question of where the GMR comes from virtually haunted the whole community since up to then only electric transport ideas about bulk systems were available. Impurity scattering, interdiffusion at interfaces, macroscopical roughness, quantum well states, confinement effects etc attained their significance as buzz-words in this field for very simple reasons: all experiments were performed on more or less perfect samples, at different temperatures, with sometimes incompatible growing conditions and so on. It took almost a decade to improve the quality of system growing, but also the quality of measurements in order to produce 'geographically' reproducible results. Quite clearly the industrial laboratories had different approaches, mostly based on chemical or metallurgical experience; after all, their aims were to produce systems suitable for reliable practical devices. Rather hesitant new theoretical concepts in dealing with electric transport in this kind of system were introduced. For a review of GMR see e.g. [2].

Since—as usual—concepts depend very much on the clarity of definitions, here first the quantum mechanical concepts of collinearity and magnetic configurations (in the context of density functional theory) are reviewed before the actual physical properties IEC and GMR are discussed. These preliminary definitions seem to be important since very often classical spin concepts are mixed up with calculational schemes based on quantum mechanical approaches. Only in the last section are the two properties, IEC and GMR, combined with each other (in order to justify the 'and' in the title).

2. Theoretical concepts

2.1. Collinearity and non-collinearity

2.1.1. 'Spinors'. Suppose one-particle (electron) wavefunctions are products of the kind

$$\begin{aligned} &\Psi(\boldsymbol{r},\sigma)=\psi(\boldsymbol{r})\phi(\sigma); \qquad \sigma\equiv m_s=\pm\tfrac{1}{2},\\ &\phi(\tfrac{1}{2})=\begin{pmatrix}1\\0\end{pmatrix}, \qquad \phi(-\tfrac{1}{2})=\begin{pmatrix}0\\1\end{pmatrix}, \end{aligned} \tag{1}$$

where obviously the $\phi(\sigma)$, $\sigma=\pm\frac{1}{2}$, are not functions, but unit vectors in a two-dimensional vector space, usually termed 'spin space':

$$(\phi(\sigma)\cdot\phi(\sigma'))=\delta_{\sigma\sigma'}. \tag{2}$$

In principle the transformation properties of $\Psi(\boldsymbol{r},\sigma)$ are conceptually very easy, since

$$R\in \mathrm{O}(3): \qquad R\Psi(\boldsymbol{r},\sigma)=\psi(R^{-1}\boldsymbol{r})\phi(\sigma)\equiv\phi(\sigma)\psi(R^{-1}\boldsymbol{r})=\phi(\sigma)D(R)\psi(\boldsymbol{r}), \tag{3}$$

where $D(R)$ is a representation of $R\in\mathrm{O}(3)$ and

$$U(R)\in SU(2): \qquad U(R)[\psi(\boldsymbol{r})\phi(\sigma)]=\psi(\boldsymbol{r})[U(R)\phi(\sigma)]. \tag{4}$$

Recalling now the definition of the vector of Pauli spin matrices,

$$\boldsymbol{\sigma}=(\sigma_x,\sigma_y,\sigma_z), \qquad \sigma_x=\begin{pmatrix}0&1\\1&0\end{pmatrix}, \qquad \sigma_y=\begin{pmatrix}0&-\mathrm{i}\\\mathrm{i}&0\end{pmatrix}, \qquad \sigma_z=\begin{pmatrix}1&0\\0&-1\end{pmatrix}, \tag{5}$$

the Hamiltonian is usually defined within the local density functional as

$$\mathcal{H}(\boldsymbol{r})=I_2(-\tfrac{1}{2}\nabla^2+V(\boldsymbol{r}))+\sigma_z B(\boldsymbol{r}), \tag{6}$$

where I_n is a $n\times n$ unit matrix and $V(\boldsymbol{r})$ is the (effective) potential. One obvious meaning of the second term on the rhs of equation (6) is that the (effective) magnetization $\boldsymbol{B}(\boldsymbol{r})$ points along an arbitrary assumed $\hat{\boldsymbol{z}}$-direction, say $\boldsymbol{n}\in\mathcal{R}_3$, i.e., is of the form

$$\boldsymbol{B}(\boldsymbol{r})=B(\boldsymbol{r})\boldsymbol{n}, \qquad n=(0,0,1). \tag{7}$$

The general form of the scalar product between $\boldsymbol{\sigma}$ and $\boldsymbol{B}(\boldsymbol{r})$ is of course given by

$$(\boldsymbol{\sigma}\cdot\boldsymbol{B}(\boldsymbol{r}))=B(\boldsymbol{r})(\boldsymbol{\sigma}\cdot\boldsymbol{\xi})=B(\boldsymbol{r})(\sigma_x\xi_x+\sigma_y\xi_y+\sigma_z\xi_z), \tag{8}$$

with $\boldsymbol{\xi}\in\mathcal{R}_3$ being a vector of unit length in an arbitrary direction.

Quite clearly by keeping in mind equations (3) and (4), a transformation of equation (6) of the kind

$$U(R)\mathcal{H}(\boldsymbol{r})U^{-1}(R)=I_2(-\tfrac{1}{2}\nabla^2+V(\boldsymbol{r}))+U(R)\sigma_z B_z(\boldsymbol{r})U^{-1}(R), \qquad U(R)\in SU(2), \tag{9}$$

really means that only the second term on the rhs of equation (9) is transformed as

$$U(R)\sigma_z B(\boldsymbol{r})U^{-1}(R)=B(\boldsymbol{r})U(R)(\boldsymbol{\sigma}\cdot\boldsymbol{n})U^{-1}(R)=B(\boldsymbol{r})(\boldsymbol{\sigma}'\cdot\boldsymbol{n}), \tag{10}$$

where

$$\boldsymbol{\sigma}' = (\sigma_x', \sigma_y', \sigma_z') = U(R)\boldsymbol{\sigma}U^{-1}(R). \tag{11}$$

Reviewing equation (10) again, it is obvious that the scalar product on the rhs of this equation can be written also as

$$(\boldsymbol{\sigma}' \cdot \boldsymbol{n}) = (\boldsymbol{\sigma} \cdot \boldsymbol{\xi}), \tag{12}$$

where—as should be noted in particular—

$$\boldsymbol{\xi} = D^{(3)}(R)\boldsymbol{n}. \tag{13}$$

$D^{(3)}(R)$ is a rotation in $\mathcal{R}_3$ such that the condition in equation (12) is met.

Since obviously a transformation in spin-space corresponds to a similarity transformation for the Pauli spin matrices, such a transformation can be viewed also as an 'induced' transformation for the orientation of $\boldsymbol{B}(\boldsymbol{r})$.

If $\mathcal{N}_0 = \{\boldsymbol{n}_i | \boldsymbol{n}_i = (0, 0, 1), \forall i\}$ denotes a set of unit vectors in the $\hat{z}$-direction centred at the sites $i = 1, 2, \ldots, N$, and the set $\mathcal{N} = \{\boldsymbol{\xi}_i\}$ specifies the actual orientations in these sites, an arbitrary pair of orientations, $\boldsymbol{\xi}_i$ and $\boldsymbol{\xi}_j$, is said to be 'parallel' to $\mathcal{N}_0$ if

$$\boldsymbol{\xi}_i = D^{(3)}(E)\boldsymbol{n}_i; \qquad \boldsymbol{\xi}_j = D^{(3)}(E)\boldsymbol{n}_j, \tag{14}$$

'antiparallel' to $\mathcal{N}_0$ if

$$\boldsymbol{\xi}_i = D^{(3)}(E)\boldsymbol{n}_i; \qquad \boldsymbol{\xi}_j = D^{(3)}(i)\boldsymbol{n}_j \tag{15}$$

and 'collinear' to $\mathcal{N}_0$ if

$$\boldsymbol{\xi}_i = D^{(3)}(E)\boldsymbol{n}_i; \qquad \boldsymbol{\xi}_j = D^{(3)}(R)\boldsymbol{n}_j; \qquad R = E \text{ or } i, \tag{16}$$

where

$$D^{(3)}(E) = I_3, \qquad D^{(3)}(i) = -I_3. \tag{17}$$

It should be recalled that $D^{(3)}(E)$ is *induced* by a transformation in spin space with

$$U(R) \equiv \begin{pmatrix} 1 & 0 \\ 0 & 1 \end{pmatrix} \longrightarrow D^{(3)}(E), \tag{18}$$

and $D^{(3)}(i)$ for example by

$$U(R) \equiv \sigma_y = \begin{pmatrix} 0 & -\mathrm{i} \\ \mathrm{i} & 0 \end{pmatrix} \longrightarrow D^{(3)}(i). \tag{19}$$

The last equation can easily be checked using the properties of the Pauli spin matrices, namely

$$U(R)U(R)^{-1} = \begin{pmatrix} 1 & 0 \\ 0 & 1 \end{pmatrix} = \sigma_y^2, \qquad \sigma_y\sigma_z\sigma_y = -\sigma_z, \tag{20}$$

from which immediately follows that also

$$U(R) \equiv \sigma_x = \begin{pmatrix} 0 & 1 \\ 1 & 0 \end{pmatrix} \longrightarrow D^{(3)}(i). \tag{21}$$

If, therefore, in equation (16) R is *induced* by an arbitrary rotation in spin space, $U(R) \neq I_2, \sigma_x, \sigma_y$, then this pair of orientations is called 'non-collinear' for short.

It should be noted that the use of $D^{(3)}(E)$ or the choice of $\boldsymbol{n}$ in equation (16) does not imply a loss of generality, since the same description applies also to a pair of orientations

$$\boldsymbol{\xi}_i = D^{(3)}(S)D^{(3)}(E)\boldsymbol{n}_i, \qquad \boldsymbol{\xi}_j = D^{(3)}(S)D^{(3)}(R)\boldsymbol{n}_j, \tag{22}$$

with $D^{(3)}(S)$ being *induced* by some rotation $U(S) \in SU(2)$. Since in equation (9) the first term on the rhs, namely $I_2(-\frac{1}{2}\nabla^2 + V(\boldsymbol{r}))$, remains unchanged for any arbitrary $U(R) \in SU(2)$, the definition of collinearity, see equation (16), is not restricted by the possible presence of a point group symmetry.

2.1.2. 'Bispinors'. By using a relativistic description within the local density functional the Hamiltonian is given by

$$\mathcal{H}(\boldsymbol{r}) = c\boldsymbol{\alpha}\cdot\boldsymbol{p} + \beta mc^2 + I_4 V(\boldsymbol{r}) + \beta\Sigma_z B(\boldsymbol{r}), \tag{23}$$

where $\boldsymbol{\alpha} = (\alpha_1, \alpha_2, \alpha_3)$,

$$\alpha_i = \begin{pmatrix} 0 & \sigma_i \\ \sigma_i & 0 \end{pmatrix}, \qquad \beta = \begin{pmatrix} I_2 & \\ & -I_2 \end{pmatrix}, \qquad \Sigma_i = \begin{pmatrix} \sigma_i & 0 \\ 0 & \sigma_i \end{pmatrix}. \tag{24}$$

The transformation properties of $\mathcal{H}(\boldsymbol{r})$ are now slightly more complicated [17]. Consider a rotation R, then invariance by R implies that

$$S(R)\mathcal{H}(R^{-1}\boldsymbol{r})S^{-1}(R) = \mathcal{H}(\boldsymbol{r}), \tag{25}$$

where $S(R)$ is a 4×4 matrix transforming the Dirac matrices α_i, β and Σ_i

$$S(R) = \begin{pmatrix} U(R) & 0 \\ 0 & \det[\pm]U(R) \end{pmatrix}, \tag{26}$$

and $U(R)$ is a (unimodular) 2×2 matrix and $\det[\pm] = \det[D^{(3)}(R)]$ with $D^{(3)}(R)$ being the corresponding three-dimensional rotation matrix. Using now the invariance condition in (25) explicitly, one can see immediately that the condition

$$S(R)[I_4 V(R^{-1}\boldsymbol{r})]S^{-1}(R) = I_4 V(R^{-1}\boldsymbol{r}) = I_4 V(\boldsymbol{r}) \tag{27}$$

yields the usual *rotational invariance* condition for the potential, while the terms

$$S(R)[c\boldsymbol{\alpha}\cdot\boldsymbol{p}]S^{-1}(R), \qquad S(R)[\beta\boldsymbol{\Sigma}\cdot\boldsymbol{B}(R^{-1}\boldsymbol{r})]S^{-1}(R), \tag{28}$$

have to be examined with more care. Considering the scalar product here explicitly term-wise, this reduces to the following common condition for both expressions in (28):

$$U(R)\boldsymbol{\sigma}U^{-1}(R) = \boldsymbol{\sigma}. \tag{29}$$

As in the previous *'spinor'* case the obvious meaning of equation (23) is that the 'magnetization' $\boldsymbol{B}(\boldsymbol{r})$ points along an arbitrary assumed $\hat{z}$-direction, i.e., is of the form

$$\boldsymbol{B}(\boldsymbol{r}) = B(\boldsymbol{r})\boldsymbol{n}, \qquad \boldsymbol{n} = (0, 0, 1). \tag{30}$$

However, by comparing now the transformation properties in the *'spinor'* and the *'bispinor' case*, one can easily see that in the *'bispinor' case* for a proper definition of collinearity an *induced* rotation for the orientation of $\boldsymbol{B}(\boldsymbol{r})$, such as defined in equations (12) and (13), is restricted by a possibly present rotational invariance condition for

(1) the (effective) potential $V(\boldsymbol{r})$,

$$V(R^{-1}\boldsymbol{r}) = V(\boldsymbol{r}), \tag{31}$$

(2) the (effective) magnetization $B(\boldsymbol{r})$,

$$B(R^{-1}\boldsymbol{r}) = B(\boldsymbol{r}), \tag{32}$$

and

(3) the invariance condition for the kinetic energy operator $c\boldsymbol{\alpha}\cdot\boldsymbol{p}$, whereby, because of the term $\beta\Sigma_z B(\boldsymbol{r})$, the sign of $\boldsymbol{\sigma}$ has to be preserved, i.e., equation (29) has to be fulfilled simultaneously.

Expressed in colloquial terms this simply means that 'spin–orbit coupling' also enters the definition of collinearity.

2.1.3. Translational properties. In the *'spinor'* case translational invariance,

$$\mathcal{H}(\boldsymbol{r}+\boldsymbol{t}) = I_2(-\tfrac{1}{2}\nabla^2 + V(\boldsymbol{r}+\boldsymbol{t})) + \sigma_z B_z(\boldsymbol{r}+\boldsymbol{t}) = \mathcal{H}(\boldsymbol{r}), \qquad t \in \mathcal{L}^{(n)}, \tag{33}$$

where $\mathcal{L}^{(n)}$ is either a three-dimensional or a two-dimensional lattice, implies—as easily can be checked—that

$$\boldsymbol{\xi}_i = \boldsymbol{\xi}_0, \qquad \forall i \in I(\mathcal{L}^{(n)}), \tag{34}$$

where $I(\mathcal{L}^{(n)})$ denotes the set of indices corresponding to $\mathcal{L}^{(n)}$ and $\boldsymbol{\xi}_0$ is some arbitrarily chosen orientation of $\boldsymbol{B}(\boldsymbol{r})$ such as for example $\hat{\boldsymbol{z}}$. Equation (34) also applies in the *'bispinor'* case, since for a translation the matrix $S(R)$ in equation (25) has to be the unit matrix, see also [17]. It should be noted that equation (33) can easily be extended to complex lattices. According to the discussions above non-collinearity can formally only be introduced by either reducing the dimensions of the lattice or, in special cases, considering complex lattices.

2.2. Magnetic configurations

Based on the previous section it is now very easy to define collinear magnetic structures in layered systems. Suppose that for a two-dimensional translational invariant system (layered system) a particular configuration

$$\mathcal{C}_i = \{\ldots, n_{k-1}, n_k, n_{k+1}, \ldots\}, \tag{35}$$

where k numbers atomic layers, is defined [17] by a set of collinear unit vectors n_k that characterize the orientations of the magnetization in all atomic layers considered, then configuration

$$\mathcal{C}_j = \{\ldots, n_{k-1}, -n_k, n_{k+1}, \ldots\} \tag{36}$$

refers to an arrangement in which with respect to $\mathcal{C}_i$ the orientation of the magnetization is reversed in the kth atomic layer. Taking also non-collinear configurations into account implies that $\mathcal{C}_j$ can be reached [17] in a continuous manner by means of a rotation $U(\Theta)$ of n_k, $0 \leqslant \Theta \leqslant 2\pi$, around an axis perpendicular to n_k, i.e., by considering configurations of the form

$$\mathcal{C}_i(\Theta) = \{\ldots, n_{k-1}, U(\Theta)n_k, n_{k+1}, \ldots\}. \tag{37}$$

This implies that although within one atomic layer because of translational symmetry collinearity has to apply, with respect to each other the various layers can be orientated non-collinearly. Restricting, however, theoretical investigations to collinear configurations demands that in all atomic layers the corresponding orientations of the magnetization are either parallel or antiparallel to a given direction. This is indeed important to recall since even in the simplest case of a ferromagnetic configuration (all orientations are parallel) the prechosen direction of reference can be in plane or perpendicular to the planes of atoms.

3. Interlayer exchange coupling and the magnetic force theorem

At a first glance it would seem that by simply taking the total energy difference between the two relevant magnetic configurations, namely the so-called ferromagnetic ('parallel') and the antiferromagnetic ('antiparallel') ones, the IEC can readily be obtained. Unfortunately this implies taking the difference between two very large numbers, i.e., one has to be sure that both total energies are well converged not only with respect to the Brillouin zone integration used but also with respect to a sufficient number of decimal places since the IEC usually is only of the order of a few millielectronvolts or even less. Independent from the actual 'band

structure' method applied this *caveat* makes the use of total energies numerically not quite advisable. Furthermore, electronic structure methods based on three-dimensional translational periodicity ('supercell approaches') can be quite misleading for essentially two reasons:

(1) in reality, i.e., in experiments, there is only a trilayer system consisting of two magnetic slabs and a spacer and not a periodic array of trilayers, and
(2) by changing for example the thickness of the spacer the Fermi energy changes, causing in turn incompatibilities with respect to the magnetic slabs.

For the latter reasons essentially only approaches based on two-dimensional periodicity ('surface Green function approaches for layered systems') guarantee a physically correct description of a system consisting of a substrate and a magnetic trilayer with a free surface, in particular since only Green function approaches are suitable for taking into account effects of alloying and interdiffusion at interfaces in terms of the coherent potential approximation.

In most applications the magnetic force theorem [3] was applied by considering only the grand potentials of the two magnetic configurations under investigation

$$\Delta E_b = E_b(\mathcal{C}) - E_b(\mathcal{C}_0), \tag{38}$$

evaluating, however, only the reference configuration ($\mathcal{C}_0$, one of them) self-consistently. If c_α^p denotes the respective concentrations of the constituents A and B in layer p then in terms of the (inhomogeneous) CPA for layered systems [15] ΔE_b is given by

$$\Delta E_b = \sum_{p=1}^{N} \sum_{\alpha=A,B} c_\alpha^p \Delta E_\alpha^p, \tag{39}$$

where the

$$\Delta E_\alpha^p = \int_{\epsilon_b}^{\epsilon_F} \Delta n_\alpha^p(\epsilon)(\epsilon - \epsilon_F)\,\mathrm{d}\epsilon, \tag{40}$$

refer to component- and layer-resolved contributions to the grand potential at $T = 0$. In equation (40) $\Delta n_\alpha^p(\epsilon)$ is the difference of the component-and layer-projected DOSs with respect to the orientation of the magnetization, ϵ_b denotes the bottom of the valence band and ϵ_F is the Fermi energy of the (nonmagnetic) substrate. Note that because of the definition given in equation (38) a positive/negative value of the IEC implies an antiparallel/parallel set-up of the orientations of the magnetization. The numerical advantage of using the grand potentials is that

(1) they can be calculated very accurately and that
(2) only differences of reasonably small numbers have to be taken.

The error made by evaluating only one magnetic configuration self-consistently is usually of the order of 3–5%, see [40].

Since in the following exclusively examples in terms of the screened KKR method [31, 46] will be shown the reader is referred to the vast number of papers [7–14, 16, 18–21, 25, 26, 30, 39] that are based on the TB-LMTO method [47] in which all kinds of effect on the IEC, from ordering to temperature effects, have been investigated.

It should be noted that the definition in (38) also applies to the so-called band energy part of the magnetic anisotropy energy [31]. In this case $\mathcal{C}$ and $\mathcal{C}_0$ refer to a uniform in-plane and a uniform perpendicular-to-the-planes-of-atoms orientation of the magnetization. It was found, e.g., that in some systems such as Cu(100)/Co_n [23] the corresponding band energy contribution oscillates with n.

4. Kubo–Greenwood type description of electric transport

In this section the main emphasis is devoted to the use of a Kubo–Greenwood description of electric transport in a magnetic multilayer system. Since this is not the only approach to deal with this problem the reader is also referred to a Kubo–Landauer-type method [29, 32–35, 41] at present in use within the TB-LMTO method.

4.1. General expressions

Suppose the electrical conductivity of a disordered system, namely $\sigma_{\mu\nu}$, is calculated using the Kubo–Greenwood formula (see [4–6, 46])

$$\sigma_{\mu\nu} = \frac{\pi\hbar}{N_0\Omega_{at}}\left\langle \sum_{m,n} J^{\mu}_{mn} J^{\nu}_{nm} \delta(\epsilon_F - \epsilon_m)\delta(\epsilon_F - \epsilon_n)\right\rangle. \tag{41}$$

In this equation $\mu, \nu \in \{x, y, z\}$, N_0 is the number of atoms, J^{ν} is a representation of the νth component of the current operator,

$$J^{\nu} = \{J^{\nu}_{nm}\}; \qquad J^{\nu}_{nm} = \langle n|J_{\nu}|m\rangle, \tag{42}$$

$|m\rangle$ is an eigenstate of a particular configuration of the random system, Ω_{at} is the atomic volume and $\langle\cdots\rangle$ denotes an average over configurations. Equation (41) can be reformulated in terms of the imaginary part of the (one-particle) Green function

$$\sigma_{\mu\nu} = \frac{\hbar}{\pi N_0\Omega_{at}} \operatorname{Tr}\langle J_{\mu}\mathrm{Im}G^{+}(\epsilon_F)J_{\nu}\mathrm{Im}G^{+}(\epsilon_F)\rangle \tag{43}$$

or, by using 'up-' and 'down-'side limits, this equation can be rewritten [5] as

$$\sigma_{\mu\nu} = \tfrac{1}{4}\{\tilde{\sigma}_{\mu\nu}(\epsilon^{+}, \epsilon^{+}) + \tilde{\sigma}_{\mu\nu}(\epsilon^{-}, \epsilon^{-}) - \tilde{\sigma}_{\mu\nu}(\epsilon^{+}, \epsilon^{-}) - \tilde{\sigma}_{\mu\nu}(\epsilon^{-}, \epsilon^{+})\}, \tag{44}$$

where

$$\epsilon^{+} = \epsilon_F + \mathrm{i}\delta, \qquad \epsilon^{-} = \epsilon_F - \mathrm{i}\delta; \qquad \delta \to 0, \tag{45}$$

and

$$\tilde{\sigma}_{\mu\nu}(\epsilon_1, \epsilon_2) = -\frac{\hbar}{\pi N_0\Omega_{at}} \operatorname{tr}\langle J_{\mu}G(\epsilon_1)J_{\nu}G(\epsilon_2)\rangle; \qquad \epsilon_i = \epsilon^{\pm}; i = 1, 2. \tag{46}$$

4.2. Two-dimensional translational invariant systems

As in the bulk case [5, 46] a typical contribution to the conductivity can be expressed in terms of real space scattering path operators [31, 46],

$$\tilde{\sigma}_{\mu\nu}(\epsilon_1, \epsilon_2) = (C/N_0)\sum_{p=1}^{n}\left\{\sum_{i\in I(L_2)}\sum_{q=1}^{n}\left\{\sum_{j\in I(L_2)} \operatorname{tr}\langle J^{pi}_{\mu}(\epsilon_2, \epsilon_1)\tau^{pi,qj}(\epsilon_1)J^{qj}_{\nu}(\epsilon_1, \epsilon_2)\tau^{qj,pi}(\epsilon_2)\rangle\right\}\right\} \tag{47}$$

where $C = -(4m^2/\hbar^3\pi\Omega_{at})$ and $N_0 = nN$ is the total number of sites in the intermediate region (actual multilayer augmented by a few layers of the substrate and the cap), as given in terms of the number of layers p, q in the multilayer (n), and the order of the two-dimensional translational group N (number of atoms in one layer). In (47) $I(L_2)$ denotes the set indices corresponding to the two-dimensional lattice L_2. This equation is of such a form that not only lattice Fourier transformations [15] can be performed, but also an inhomogeneous CPA can

be applied [15]. One finally obtains the following relation for the diagonal elements of the conductivity tensor:

$$\sigma_{\mu\mu}(n;\boldsymbol{c};\mathcal{C}) = \lim_{\delta\to 0}\sigma_{\mu\mu}(n;\boldsymbol{c};\mathcal{C};\delta), \qquad \sigma_{\mu\mu}(n;\boldsymbol{c};\mathcal{C};\delta) = \frac{1}{n}\sum_{p,q=1}^{n}\sigma_{\mu\mu}^{pq}(\boldsymbol{c};\mathcal{C};\delta), \tag{48}$$

where δ refers to the imaginary part of the Fermi energy and $\mathcal{C}$ to the chosen magnetic configuration and the vector $\boldsymbol{c}$ contains the layer-wise concentrations of species A and B, c_α^p, of a possibly inhomogeneous alloyed layered system.

4.2.1. Current-in-plane geometry. In the case of a current-in-plane (CIP) geometry the resistivity is then simply given [36] by

$$\rho_{\mu\mu}(n;\boldsymbol{c};\mathcal{C}) = \lim_{\delta\to 0}\rho_{\mu\mu}(n;\boldsymbol{c};\mathcal{C};\delta), \qquad \rho_{\mu\mu}(n;\boldsymbol{c};\mathcal{C};\delta) = 1/\sigma_{\mu\mu}(n;\boldsymbol{c};\mathcal{C};\delta), \tag{49}$$

and was used for quite a few systems such as permalloy [36] or Fe/Cr/Fe [40] and Co/Cu/Co [42] spin valve systems.

4.2.2. Current-perpendicular-to-the-planes geometry. For a current-perpendicular-to-the-planes (CPP) geometry the sheet resistance for a particular magnetic configuration can be obtained from the following set of equations [37]:

$$\sum_{q=1}^{n}\rho_{pq}(n;\boldsymbol{c};\mathcal{C};\delta)\sigma_{qp}(n;\boldsymbol{c};\mathcal{C};\delta) = \delta_{pq} \tag{50}$$

$$r(n;\boldsymbol{c};\mathcal{C};\delta) = \sum_{p,q=1}^{n}\rho_{pq}(n;\boldsymbol{c};\mathcal{C};\delta) \tag{51}$$

$$r(n;\boldsymbol{c};\mathcal{C}) = \lim_{\delta\to 0} r(n;\boldsymbol{c};\mathcal{C};\delta) \tag{52}$$

such that

$$|r(n+m;\boldsymbol{c};\mathcal{C}) - r(n;\boldsymbol{c};\mathcal{C})| < \Delta; \qquad n,m\in\mathbb{N}^+, \tag{53}$$

where Δ is an infinitesimally small number. This approach has been successfully applied to Fe/Ge/Fe [37] and Fe/ZnSe/Fe [38] heterostructures.

4.2.3. Giant magnetoresistance. The giant magnetoresistance is finally is defined by the ratio

$$MR(n;\boldsymbol{c}) = \frac{R(n;\boldsymbol{c};\mathcal{C}_1) - R(n;\boldsymbol{c};\mathcal{C}_0)}{R(n;\boldsymbol{c};\mathcal{C}_1)}, \tag{54}$$

$$R(n;\boldsymbol{c};\mathcal{C}) = \begin{cases} \rho(n;\boldsymbol{c};\mathcal{C}); & \text{CIP} \\ r(n;\boldsymbol{c};\mathcal{C}); & \text{CPP,} \end{cases} \tag{55}$$

where $\mathcal{C}_1$ refers to the antiferromagnetic and $\mathcal{C}_0$ to the ferromagnetic configuration. The advantage of using this kind of definition is simply that $MR(n;\boldsymbol{c}) \leqslant 1$.

5. Dangers, applications and illustrations

5.1. What is the correct antiferromagnetic configuration?

Consider for simplicity a typical trilayer system deposited on a non-magnetic substrate of orientation (hkl), i.e. the system $substrate(hkl)/M_1/S/M_2/Vac$, with M_1 and M_2 denoting two magnetic slabs of thickness (in monolayers) m_1 and m_2, and S referring to a spacer of

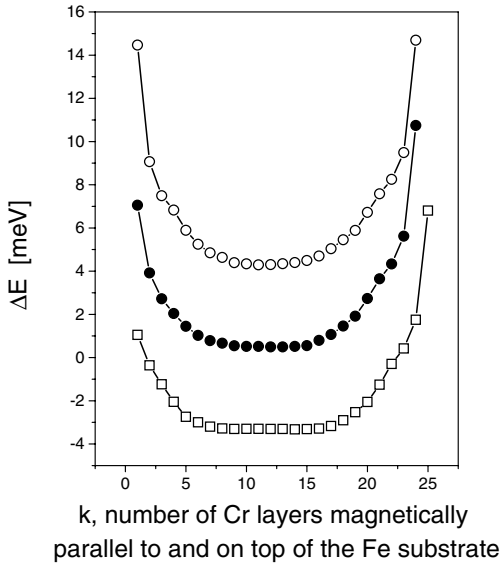

Figure 1. Interlayer exchange energy for bcc-Fe(100)/$Fe_6Cr_nFe_6$/Vac for $n = 24$ (open circles) and $n = 25$ (open squares) with respect to an increasing number k of Cr layers on top of and aligned magnetically parallel to the Fe substrate. Full circles correspond to the bias (from [48]).

thickness s. Clearly enough depending on the kind of material used for M_1 and M_2 and their respective thicknesses a ferromagnetic configuration refers to a uniform orientation of the magnetization either perpendicular ('in plane') or parallel ('perpendicular to the planes of atoms') to the surface normal. Less clear is the definition of 'the' antiferromagnetic configuration, since the spacer material can be partially or even totally magnetized. Suppose s_1 and s_2 represent the numbers of magnetized spacer layers in the vicinity of the left-and the right-hand interface in the above example. As long as $(s_1 + s_2) < s$ the antiferromagnetic configuration with respect to a given ferromagnetic configuration is simply defined by reversing the orientation of the magnetization in either the (m_1+s_1) atomic layers on top of the substrate, or the $(m_2 + s_2)$ layers of the system interfacing vacuum. Very small differences in the IEC corresponding to these two cases can occur and can be caused by whether or not M_1 and M_2 are formed by the same material. If, however, $(s_1 + s_2) = s$ then difficulties can arise whether s is even or odd. In the case of an even number of magnetized spacer layers the orientation of the magnetization can be reversed either in the first half $(m_1 + s_1)$ layers of the multilayer system or in the second half $(m_2 + s_2)$. In the case of an odd number of spacer layers either $(m_1 + s_1) > (m_2 + s_2)$ or $(m_1 + s_1) < (m_2 + s_2)$. Both cases, namely when the orientation of the magnetization in half of the spacer is reversed simultaneously, are usually termed a 'symmetric' antiferromagnetic configuration.

A famous case of a magnetized spacer is the system bcc-Fe(100)/Cr_s/Fe_{s_2} [38]. In figure 1 the IEC in this system is shown for $s = 24$ and 25 as a function of the number of Cr layers parallel to the orientation of the magnetization in M_1. As can be seen there is a kind of bias (defined in this particular case as the arithmetic mean of the top and the bottom curve) around which the IEC will oscillate. This bias is not zero since $m_2 \ll m_1$, for details see [38].

The oscillations of the IEC corresponding to the 'symmetric' antiferromagnetic configuration $(m_1 + s_1) \leqslant (m_2 + s_2)$ are shown in figure 2. Also displayed in this figure is the case of perpendicular exchange coupling. One can easily read off from this figure two

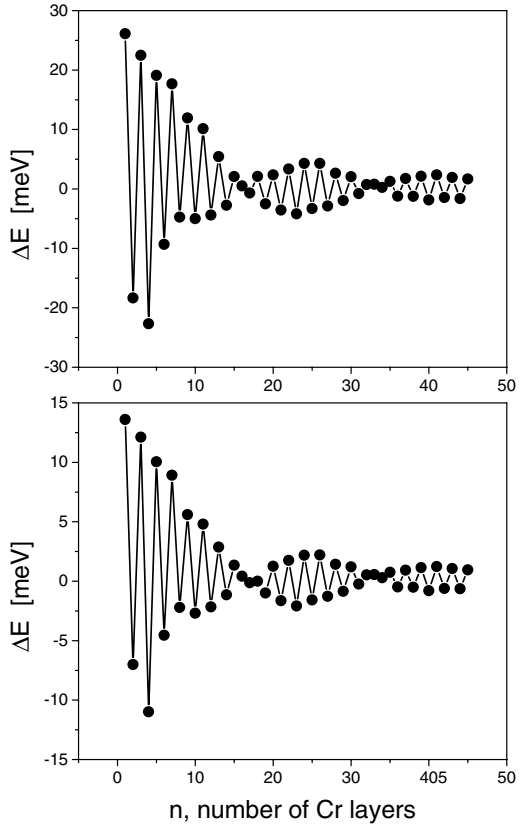

Figure 2. Antiparallel (top) and perpendicular (bottom) IEC in bcc-Fe(100)/$Fe_6Cr_nFe_6$/Vac (from [48]).

periods of oscillations, namely a short period of two monolayers (MLs) and a long period of about 16–17 ML, and even see the famous 'phase slip'.

It should be noted that the examples shown here are meant to draw attention to the fact that the IEC is by no means an easy property to describe. Even in cases when no interdiffusion at interfaces has to be taken into account, exactly the same sample characteristics as in experiment have to be reproduced in the theoretical descriptions, since otherwise any comparison with experimental data becomes useless.

5.2. Does the GMR have the same kind of oscillation as the IEC?

This question was posed right from the beginning and it seemed to be obvious by intuition, since the resistivity of an antiferromagnetic arrangement is said to be larger than of a ferromagnetic arrangement. As can be seen from figure 3 in CIP the resistivity of the bcc-Fe(100)/$Fe_6Cr_nFe_6$/Vac system shows a period of 3–4 ML which, however, is not mapped in the corresponding IEC, see figure 2; the phase slips at 15 and 30 ML on the other hand can be traced also in the GMR as at these thicknesses the GMR vanishes or even changes sign.

Alloying of the spacer homogeneously can have drastic effects [42]: as can be seen from figure 4 in Co/Cu/Co spin valves small amounts of Ti or Pd (Pt) can reduce the GMR considerably or even whip out the whole effect. The effect of interdiffusion is illustrated

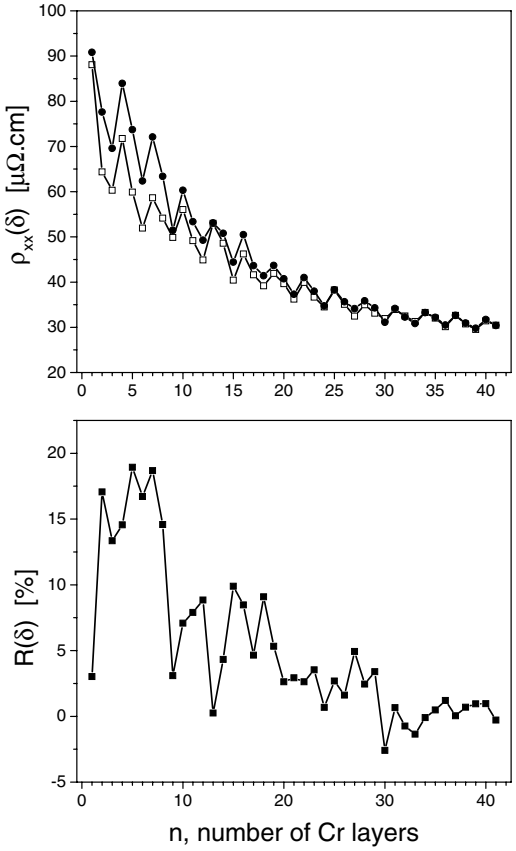

Figure 3. CIP electric transport: parallel (open squares) and antiparallel (full circles) in-plane resistivities (top) and magnetoresistance (bottom) of bcc-Fe(100)/$Fe_6Cr_nFe_6$/Vac, $n \leqslant 42$. The imaginary part δ of the complex Fermi energy $\epsilon_F + \mathrm{i}\delta$ is 2 mRyd.

in figure 5, in which several interdiffusion profiles for a particular Co/Cu/Co spin valve are considered (for further details, see [42]).

The question of where the GMR in the case of a CPP geometry is coming from can be best illustrated using layer-resolved sheet resistance differences, see equation (51),

$$r_p(n; \boldsymbol{c}; \mathcal{C}; \delta) = \sum_{q=1}^{n} \rho_{pq}(n; \boldsymbol{c}; \mathcal{C}; \delta) \tag{56}$$

and performing the sum over the layers in relevant parts such as leads (L_{left}, L_{right}), a few layers forming the interfaces (I_{left}, I_{right}) and the spacer (S).

$$\Delta r(n; \boldsymbol{c}; \mathcal{AP}; \delta) \equiv \sum_{p=1}^{n} r_p(n; \boldsymbol{c}; \mathcal{AP}; \delta) - r_p(n; \boldsymbol{c}; \mathcal{P}; \delta) = \Delta r_{L_{left}}(n; \boldsymbol{c}; \delta) + \Delta r_{L_{right}}(n; \boldsymbol{c}; \delta)$$
$$+ \Delta r_{I_{left}}(n; \boldsymbol{c}; \delta) + \Delta r_{I_{right}}(n; \boldsymbol{c}; \delta) + \Delta r_S(n; \boldsymbol{c}; \delta). \tag{57}$$

This procedure is used in figure 6 for a particular Fe/ZnSe/Fe heterostructure. As can be seen for both kinds of termination the GMR effect is caused by the interfaces. For details see [38].

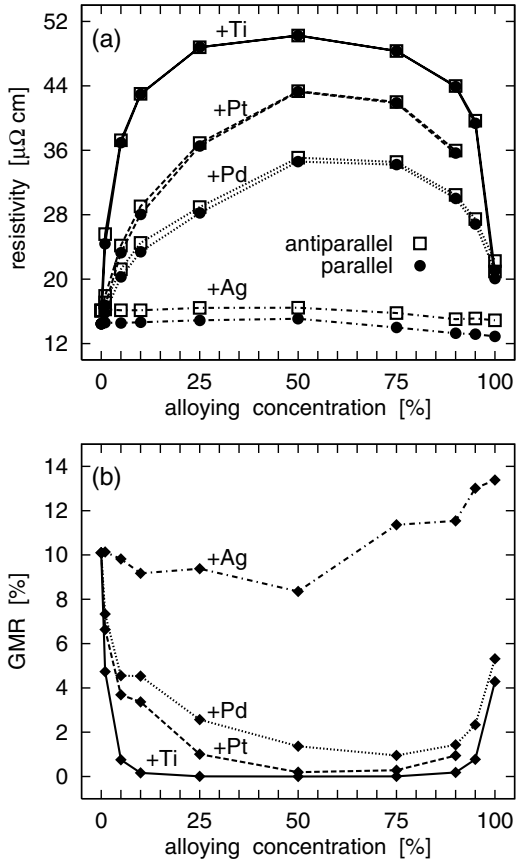

Figure 4. (a) Resistivities and (b) GMR for a model spin-valve structure with homogeneously alloyed Cu spacer layers Co(100)/$Co_{12}(Cu_{100-c}X_c)_{12}Co_{12}$/Co(100) with $\delta = 2$ mRyd and with outgoing boundary conditions. X = Ag (dash–dotted curves), Pd (dotted curves), Pt (dashed curves) or Ti (solid curves). Resistivities for the antiparallel configuration are displayed by open squares, resistivities for the parallel configuration by full circles (from [49]).

6. IEC and GMR

In principle, if $\mathcal{C}_0$ denotes the collinear ground state, one can view [43] the MR as an implicit function of the exchange coupling energy ϵ,

$$\begin{aligned} &\epsilon = E_b(\mathcal{C}) - E_b(\mathcal{C}_0) \geqslant 0, \\ &R(\epsilon) = \frac{r(\mathcal{C}_0) - r(\epsilon)}{r(\mathcal{C}_0)}, \end{aligned} \tag{58}$$

where in CPP $r(\epsilon)$ is that sheet resistance (resistivity in the case of CIP) which (with respect to $\mathcal{C}_0$) corresponds to a magnetic configuration of interlayer exchange energy ϵ. Clearly enough for certain regimes of ϵ the magnetoresistance $R(\epsilon)$ remains constant while in other regimes rapid changes with ϵ occur: the interlayer exchange energy ϵ acts like a magnetic field (external energy) that is switched on continuously. Increasing ϵ 'forces' the system to gradually assume the magnetic configuration with the next highest energy, etc. Consequently one can define the exchange bias E_{bias} in terms of $R(\epsilon)$ in the following manner:

$$0 \leqslant \epsilon \leqslant E_{bias} : R(\epsilon) = 0; \qquad \epsilon > E_{bias} : R(\epsilon) \neq 0. \tag{59}$$

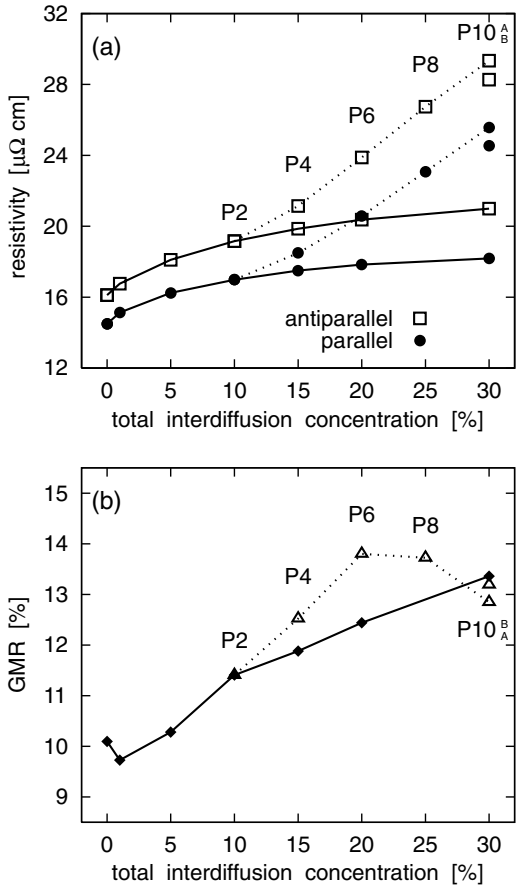

Figure 5. (a) Resistivities and (b) GMR as a function of interdiffusion amount and profile for the model spin-valve structure Co(100)/$Co_{12}Cu_{12}Co_{12}$/Co(100) with $\delta = 2$ mRyd. Resistivities for the antiparallel configuration are displayed by open squares, resistivities for the parallel configuration by full circles. The solid curves connect the values corresponding to interdiffusion confined to the two ML adjacent to the interface; the dotted curves connect the various broader profiles (from [42]).

Obviously for all $\epsilon \leqslant E_{bias}$ it is sufficient to consider only collinear configurations, while for $\epsilon > E_{bias}$ also particular non-collinear configurations have to be taken into account. It should be noted that of course this definition applies only to systems for which a recordable change in the MR can be observed, e.g., in spin-valve systems with an AF part.

In figure 7 the ten lowest collinear interlayer exchange energies and the corresponding MR (CIP and CPP) are shown for Co(111)/Co_6/$(CoO)_n$/Co_6/Cu_6/Co_6/Co(111), $n = 6, 12$. Although the interlayer exchange energy increases for the first seven (collinear) configurations the MR remains zero and only jumps suddenly between configurations C_7 and C_8. This jump between configurations C_7 and C_8 is characteristic for both thicknesses of the CoO part of the system. The 'flip energy' E_{flip} that causes the jump in the MR can be defined as the difference between E_{bias} and the closest larger collinear interlayer exchange energy (C_8 in the present case). In the present case this energy amounts to 0.416 meV for $n = 6$ and 0.399 meV for $n = 12$. In order to give a rough estimate in kOe, by using the relation $\Delta E = \mu_B B$ (1 meV = 172.76 kOe), these energies amount to 72 and 69 kOe, respectively.

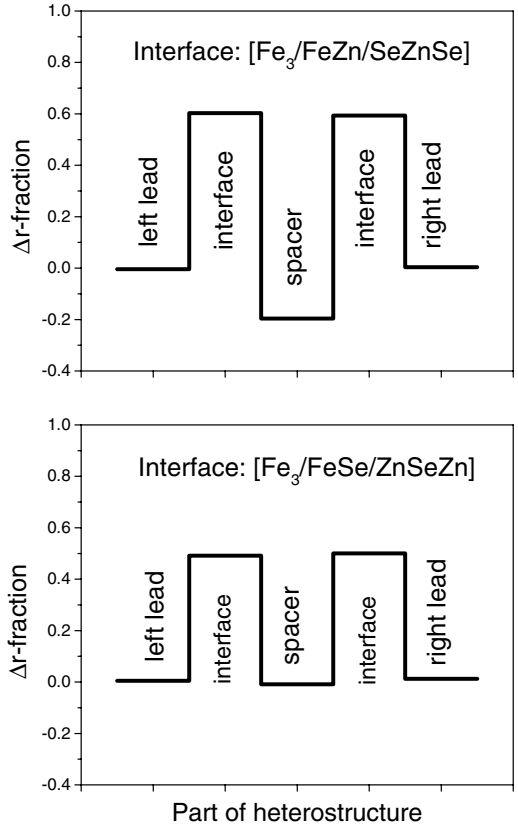

Figure 6. Normalized fractions of the difference in the sheet resistance between the antiferromagnetic and the ferromagnetic configuration in Fe(100)/$(ZnSe)_{21}$/Fe(100). The various regions of the heterostructure are given explicitly (from [38]).

E_{bias} is caused by two different types of effect, namely

(1) a rearrangement of the orientations of the magnetization in the oxygen layers and
(2) a rearrangement of orientations in the Cu spacer layers.

For $n \geqslant 6$ E_{bias} depends only very weakly on the thickness of the CoO part of the system and amounts to about 0.035 meV (6 kOe, see the above relation). In table 1 of [44] the maximum reported value of the exchange bias for Co–CoO materials is listed as 9.5 kOe; the agreement with experiment is therefore reasonably good. For further details, see [43].

7. Summary

It was the aim of this paper to review certain theoretical aspects of the interlayer exchange energy and the GMR, emphasizing in particular the concept of magnetic configurations. Many important ingredients of a more complete theoretical description of these phenomena are still missing: effects of finite temperature, macroscopical roughness at interfaces, the problem of vertex corrections in the case of electric transport etc. However, it is quite encouraging to see results of careful experiments and of carefully conducted theoretical calculations agree within

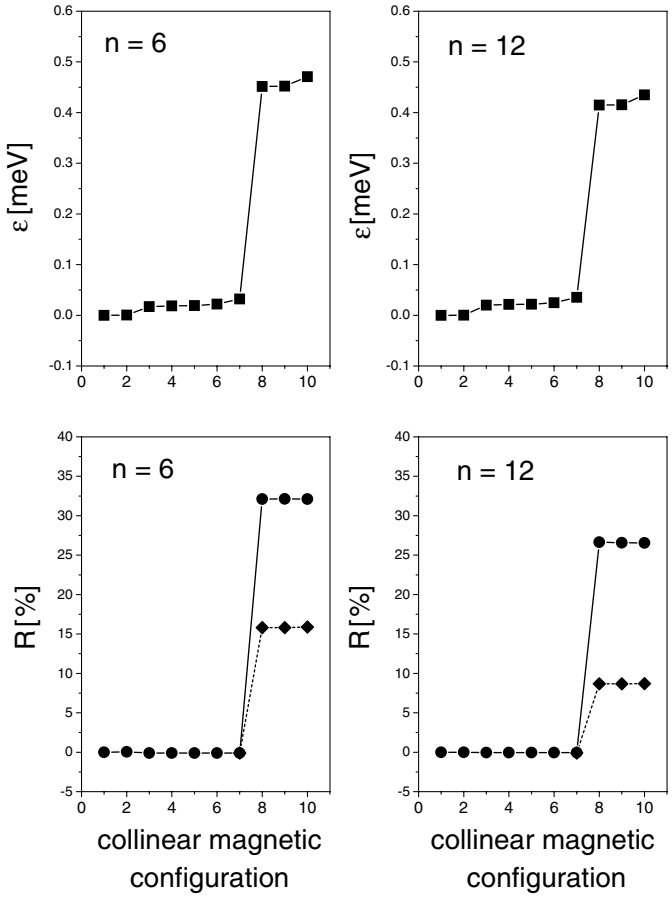

Figure 7. The ten lowest interlayer exchange energies and corresponding magnetoresistances. CPP and CIP are denoted by circles and diamonds, respectively. The number of repetitions of a CoO double layer is marked explicitly (from [43]).

a factor of two to five. This indeed is almost miraculous when comparing [45] conductivities or resistivities (absolute numbers) in such complicated systems as spin valves.

Acknowledgments

This work has been partially funded by the RTN network 'Magnetoelectronics' (contract No RTN1-1999-00145) and by the Austrian science ministry (BM:bwk GZ45.504). Financial support was provided by the Hungarian National Science Foundation (contract No OTKA T030240 and T037865).

References

[1] Potter C D, Schad R, Belien P, Verbanck G, Moshchalkov V V, Brunynseraede Y, Schäfer M, Schäfer R and Grünberg P 1994 *Phys. Rev.* B **49** 16055
[2] Tsymbal E Y and Pettifor D G 2001 *Solid State Phys.* **56** 113–237
[3] Jansen H J F 1999 *Phys. Rev.* B **59** 4699

[4] Kubo R 1957 *J. Phys. Soc. Japan* **12** 570
Greenwood D A 1958 *Proc. Phys. Soc.* **71** 585
[5] Butler W H 1985 *Phys. Rev.* B **31** 3260
[6] Banhart J, Ebert H, Weinberger P and Voitländer J 1994 *Phys. Rev.* B **50** 2104
[7] Kudrnovský J, Drchal V, Turek I and Weinberger P 1994 *Phys. Rev.* B **50** 16105
[8] Kudrnovský J, Drchal V, Turek I and Weinberger P 1995 *J. Magn. Magn. Mater.* **140–144** 511
[9] Turek I, Kudrnovský J, Šob M, Drchal V and Weinberger P 1995 *Phys. Rev. Lett.* **74** 2551
[10] Kudrnovský J, Drchal V, Turek I, Sob M and Weinberger P 1996 *J. Magn. Magn. Mater.* **156** 245
[11] Kudrnovský J, Drchal V, Turek I, Sob M and Weinberger P 1996 *Phys. Rev.* B **53** 5125
[12] Drchal V, Kudrnovský J, Turek I and Weinberger P 1996 *Phys. Rev.* B **53** 15036
[13] Kudrnovský J, Drchal V, Blaas C, Turek I and Weinberger P 1996 *Phys. Rev. Lett.* **76** 3834
[14] Kudrnovský J, Drchal V, Bruno P, Turek I and Weinberger P 1996 *Phys. Rev.* B **54** R3738
[15] Weinberger P, Levy P M, Banhart J, Szunyogh L and Úfalussy B 1996 *J. Phys.: Condens. Matter* **8** 7677
[16] Kudrnovsky J, Drchal V, Coehoorn R, Sob M and Weinberger P 1997 *Phys. Rev. Lett.* **78** 358
[17] Weinberger P 1997 *Phil. Mag.* B **75** 509
[18] Kudrnovský J, Drchal V, Turek I, Šob M and Weinberger P 1997 *Acta Phys. Polon.* A **91** 15
[19] Kudrnovský J, Drchal V, Turek I and Weinberger P 1997 *Comput. Mater. Sci.* **8** 87
[20] Kudrnovský J, Drchal V, Bruno P, Coehoorn R, De Vries J J, Wildberger K, Dederichs P H and Weinberger P 1997 *MRS Symp. Proc.* vol 475, ed J Tobin *et al* (Pittsburgh, PA: Materials Research Society) p 575
[21] Kudrnovský J, Drchal V, Bruno P, Turek I and Weinberger P 1997 *Phys. Rev.* B **56** 8919
[22] Weinberger P, Sommers C, Pustogowa U, Szunyogh L and Újfalussy B 1997 *J. Physique* I **7** 1299
[23] Szunyogh L, Úfalussy B, Blaas C, Pustogowa U, Sommers C and Weinberger P 1997 *Phys. Rev.* B **56** 14036
[24] Kudrnovský J, Drchal V, Bruno P, Turek I and Weinberger P 1998 *Comput. Mater. Sci.* **10** 188
[25] Drchal V, Kudrnovsky J, Bruno P, Dederichs P H and Weinberger P 1998 *Phil. Mag.* B **78** 571
[26] Drchal V, Kudrnovský J, Bruno P, Dederichs P H and Weinberger P 1999 *Phys. Rev.* B **60** 9588
[27] Blaas C, Weinberger P, Szunyogh L, Kudrnovsky J, Drchal V, Levy P M and Sommers C 1999 *Eur. Phys. J.* B **9** 245
[28] Blaas C, Weinberger P, Szunyogh L, Levy P M and Sommers C 1999 *Phys. Rev.* B **60** 492
[29] Kudrnovsky J, Drchal V, Turek I, Blaas C, Weinberger P and Bruno P 1999 *Czech. J. Phys.* **40** 1583
[30] Kudrnovský J, Drchal V, Bruno P, Dederichs P H and Weinberger P 2000 *Electronic Structure and Physical Properties of Solids. The Uses of the LMTO Method* ed H Dreyssé (Berlin: Springer)
[31] Weinberger P and Szunyogh L 2000 *Comput. Mater. Sci.* **17** 414
[32] Kudrnovsky J, Drchal V, Blaas C and Weinberger P 2000 *Phys. Rev.* B **62** 15084
[33] Kudrnovsky J, Drchal V, Turek I, Blaas C and Weinberger P 2000 *J. Met.* **52** 29
[34] Kudrnovsky J, Drchal V, Turek I, Blaas C, Weinberger P and Bruno P 2000 *Surf. Sci.* **454–456** 918
[35] Kudrnovsky J, Drchal V, Blaas C, Weinberger P, Turek I and Bruno P 2000 *Properties of Complex Inorganic Solids* ed A Meike, A Gonis, P E A Turchi and K Rajan (New York: Kluwer) pp 343–65
[36] Blaas C, Szunyogh L, Weinberger P, Sommers C and Levy P M 2001 *Phys. Rev.* B **63** 224408
[37] Weinberger P, Szunyogh L, Blaas C and Sommers C 2001 *Phys. Rev.* B **64** 184429
[38] Herper H C, Weinberger P, Vernes A, Szunyogh L and Sommers C 2001 *Phys. Rev.* B **64** 184442
[39] Kudrnovsky J, Drchal V, Turek I, Bruno P and Weinberger P 2001 *J. Phys.: Condens. Matter* **13** 8539
[40] Vernes A, Weinberger P, Mohn P, Blaas C, Szunyogh L, Sommers C and Levy P M 2002 *Phil. Mag.* B **82** 85–104
[41] Turek I, Kudrnovsky J, Drchal V, Szunyogh L and Weinberger P 2002 *Phys. Rev.* B **65** 125101
[42] Blaas C, Szunyogh L, Weinberger P, Sommers C, Levy P M and Shi J 2002 *Phys. Rev.* B **65** 134427
[43] Weinberger P 2002 *Phys. Rev.* B **65** 014430
[44] Nogués J and Schuller I K 1999 Exchange bias *J. Magn. Magn. Mater.* **192** 203
[45] Weinberger P and Szunyoigh L 2002 *Phys. Rev.* B **66** 144447
[46] Weinberger P 1990 *Electron Scattering Theory for Ordered and Disordered Matter* (Oxford: Clarendon)
[47] Turek I, Drchal V, Kudrnovský J, Šob M and Weinberger P 1997 *Electronic Structure of Disordered Alloys, Surfaces and Interfaces* (Dordrecht: Kluwer)
[48] Vernes A *et al* 2002 *Phil. Mag.* B **65** 85
[49] Blaas C *et al* 2002 *Phys. Rev.* B **65** 104441